Influences from the C 1*s* shape resonance on the vibrational progression in the Auger decay of CO

S. Sundin,[1,*] A. Ausmees,[1,†] O. Björneholm,[1] S. L. Sorensen,[2] M. Wiklund,[2] A. Kikas,[3] and S. Svensson[1]
[1]*Department of Physics, Uppsala University, Box 530, S-751 21 Uppsala, Sweden*
[2]*Department of Synchrotron Radiation Research, Institute of Physics, Lund University, Box 118, S-22100 Lund, Sweden*
[3]*Institute of Physics, University of Tartu, Riia 142, EE-2400 Tartu, Estonia*
(Received 10 October 1997; revised manuscript received 6 February 1998)

Auger decay from the C 1*s* core-ionized state of CO has been studied with vibrational resolution both at the C 1*s* shape resonance and far above. Variations in the vibrational intensity distribution with photon energy are observed. This observation is explained solely by the modified vibrational envelope of the core-ionized intermediate state at the shape resonance maximum, as demonstrated in a numerical simulation. This implies that the temporary trapping of the photoelectron at the shape resonance does not significantly affect the deexcitation process. Thus the deexcitation step is described by the Franck-Condon principle even at the shape resonance. The angular anisotropy of the Auger decay at the shape resonance has also been studied with vibrational resolution. Weak dependence upon the final state and no detectable influence from the vibrational quanta is observed. [S1050-2947(98)03409-X]

PACS number(s): 33.80.Eh, 32.80.Hd

I. INTRODUCTION

Vibrational branching ratios in Auger and photoelectron spectra of small molecules are typically well reproduced by the Franck-Condon principle. However, close to the threshold deviations from the Franck-Condon population may occur in valence-shell and core photoionization [1–5]. Typically these non-Franck-Condon effects are induced by shape resonances, which are located within ≈ 30 eV from threshold. Modification of vibrational populations in the Auger decay spectrum has not yet been demonstrated. This is presumably due to the experimental difficulties related to such a study; for instance, the combination of high Auger electron kinetic energy with high (vibrational) resolution has only recently become possible.

Several theoretical studies have dealt with the effects induced by the trapping of the photoelectron by the shape resonance potential. The studies have mainly been carried out using two approaches: the multiple-scattering approach where the close connection to NEXAFS of solids and adsorbate is emphasized [6], and the more generally adopted approach in which the shape resonance is described by a resonant trapping of the photoelectron in a centrifugal barrier. For *K*-shell photoionization of diatomic molecules, the shape resonance gives rise to a large increase in the σ_u continuum channel [7,8]. Therefore the shape resonance is commonly referred to as an antibonding σ^* molecular orbital in the continuum. Due to the quasibound nature of the shape resonance the coupling between the vibrational and electronic motion is enhanced, thus leading to a non-Franck-Condon population of vibrational levels [8].

Shape resonances may also affect other experimental observables. For instance, the angular distribution of ion yield, photoelectrons, and Auger electrons is known to vary over the shape resonance. This has been widely studied at both the core and valence ionization thresholds [2,4,9–11]. For valence ionization, the location of the shape resonance is typically some 1–4 eV from the corresponding core ionization shape resonance. Together with shape-resonance-enhanced continuum-continuum interchannel coupling [12] this indicates that the usual one-electron description is not sufficient for all systems, and that the shape resonance depends sensitively upon the details of the molecular potential.

From both the experimental and the theoretical side, non-Franck-Condon population of vibrational levels is well established for direct photoionization at photon energies close to the shape resonance. But, to our knowledge, no study has dealt with the influence of the shape resonance on the deexcitation processes. In a two-step description of the Auger process, the core-ionized state is the initial state of the deexcitation step and, consequently, a modified population of vibrational levels in the core-ionized state should also affect the vibrational progression in the Auger decay spectrum. However, in contrast to photoionization, it is still an open issue whether the deexcitation step at the shape resonance is described within the Franck-Condon principle. As mentioned earlier, the shape resonance is usually regarded as a temporary trapping of the outgoing photoelectron. In a qualitative picture the trapping could be regarded in one of two different extremes. If the trapping is short compared to the lifetime of the core-ionized state, deexcitation will occur predominantly after the release of the photoelectron. In this case deexcitation will not be influenced by the temporarily trapped photoelectron and the Auger spectrum can be explained simply by a modified vibrational progression in the core-ionized intermediate state. At the other extreme the trapping is comparable to the lifetime so that the deexcitation step is modified by the coupling between the vibronic/electronic motion. This implies that the deexcitation step should also be non-Franck-

*Also at University College of Gävle-Sandviken, S-801 76 Gävle, Sweden.
†Also at Institute of Physics, University of Tartu, Riia 142, EE-2400 Tartu, Estonia.

Condon. In this case one does not expect the Auger decay spectrum to be explained by a modified vibrational progression of the core-ionized intermediate state since the influences on the deexcitation must also be taken into account. As mentioned such a ''time-dependent'' analysis is only qualitative and in a more correct description a proper account of the time delay of the scattering quantities is necessary. It is also unclear to what extent the core-hole lifetime is affected by the presence of the shape resonance. In this study we will investigate if the shape-resonance-modified Auger decay spectrum can be treated by a modified population of vibrational levels in the core-ionized state alone, or, if a more elaborate method involving a non-Franck-Condon deexcitation is necessary. To do this, a numerical simulation, in which only the ionization step is non-Franck-Condon, will be compared to experimentally obtained spectra.

Previous experimental studies have shown that the angular asymmetry parameter β for transitions to various final electronic states varies over the shape resonance [9,10]. However, when both vibrational and angular resolution is available it is possible to check if the finer details of a Auger decay spectrum vary within a particular final electronic state. Within the dipole approximation the angular distribution of the emitted electrons for completely linearly polarized light is expressed as [13]

$$I(\sigma,\theta)=\frac{\sigma}{4\pi}\left[1+\frac{\beta}{2}\left(\frac{1}{2}+\frac{3}{2}\cos 2\theta\right)\right]. \tag{1}$$

Here σ is the total cross section, β is the angular anisotropy parameter of a specific transition, and θ is the angle between the electric field vector of the incoming photon beam and the direction of the emitted electron. Using this formula, we have determined the β parameter for transitions to various final states from the core-ionized intermediate state at the C $1s$ shape resonance.

II. EXPERIMENT

The measurements have been carried out at the MAX I storage ring in Lund, Sweden, at beam line 51 (BL51) [14]. The beam line uses radiation from a short-period undulator providing usable photon flux in the 60–600 eV range. A modified SX-700 plane-grating monochromator is installed at the beam line. BL51 incorporates an end station with the possibility of rotating an SES-200 electron-energy analyzer in a plane perpendicular to the direction of the incoming photon beam [15]. In this study spectra were recorded at 0° and 54.7° with respect to the electric field vector of the photons. Due to the high degree of linear polarization of the light ($>97\%$ [16]) vibrational branching ratios can be extracted directly from the spectra recorded at 54.7°. The C $1s$ core photoelectron spectra were recorded with a photon bandwidth and electron spectrometer resolution of ≈ 70 meV, respectively. This gives a total experimental resolution of ≈ 100 meV. For normal Auger decay linewidths are independent of the excitation profile, however, for the purpose of energy selectivity, a monochromator setting giving a photon bandwidth of ≈ 0.8 eV was used. Due to the high kinetic energy of the Auger electron, a Doppler broadening of ≈ 40 meV was added to the spectrometer resolution of ≈ 100 meV giving a total experimental broadening of ≈ 110 meV. The CO gas was commercially obtained with a purity of $\approx 99.9\%$.

III. CALCULATIONS

In this study we treat the Auger effect as a nonradiative scattering process and use the same formalism as for resonant Raman scattering (RRS) processes. This is possible because these processes are closely related [17,18]. For excitations with photon energies well above threshold, the Auger process is well described within a two-step model and any extra photon energy in excess of the energy needed to create the core hole will be transferred to the photoelectron. We assume no interaction between the photoelectron and the Auger electron in the continuum neglecting the postcollision interaction effect (PCI) in the calculations. Within the scattering description of the Auger effect, the vibrational intensities for transitions to a final electronic state is given by the double differential cross section:

$$\sigma_f(\hbar\omega)=\sum_{n_f}|F_{n_f}|^2\Phi(\hbar\omega), \tag{2}$$

where Φ is the unit-normalized spectral function of the exciting radiation, n_f is the vibrational quantum number of the final state, F_{n_f} are the transition amplitudes, and $\hbar\omega$ the excitation energy. Here we consider the special case of Auger decay from a core-ionized intermediate state. This is accounted for by an excitation profile Φ, which is constant over a wide energy range covering all important vibrational levels.

The transition amplitudes F_{n_f} between the ground state and the two-hole $(2h)$ final states are given by

$$F_{n_f}=\sigma_0\sum_{n_i}\frac{\langle n_f|n_i\rangle\langle n_i|n_o\rangle}{\hbar\omega-(E_n-E_0)+\imath\Gamma}. \tag{3}$$

Here all unessential constants are collected in σ_0, Γ is the intermediate-state lifetime broadening (half width at half maximum), E_n are the vibrational energies of the intermediate state, and E_0 is the energy of the ground state. Using this scattering formalism the effects of lifetime vibrational interference (LVI) are fully accounted for [19]. The calculated intensities are summed according to the monochromator excitation function on an electron emission-energy scale given by

$$\sigma(E_{\mathrm{emi}})=\sum_f\sigma_f[\hbar\omega-(E_f-E_0)], \tag{4}$$

where σ_f is the relative cross section for transitions to a certain final state (it is assumed that σ_f is the same at the shape resonance and above the shape resonance). A more detailed description of the calculation method can be found in Ref. [19]. For diatomic molecules at room temperature, the ground state is almost completely populated in the lowest vibrational level [20]. Also, from the potential curves of the ground and core-ionized states in Ref. [21], it is observed that the ground-to-intermediate state transition matrix elements are alternately positive and negative, provided that the

TABLE I. Spectroscopic constants used for calculations of the Morse potential curves.

	ω_e (cm^{-1})	$\omega_e x_e$ (cm^{-1})	R_e (Å)
CO GS	2203.8	14.09	1.129
$CO^{1+}(C\ 1s^{-1})$	2599.0	15.92	1.073
$CO^{2+}(X^1\Sigma)$	1878.5	17.15	1.170
$CO^{2+}(A^1\Pi)$	1463.8	14.13	1.257
$CO^{2+}(B^2\Sigma^+)$	2491.9	111.6	1.097

ground state is populated in the lowest vibrational level. The alternately positive and negative transition matrix elements stem from the reduction of the internuclear equilibrium distance in the core-ionized state compared to the ground state and the fact that both of these states are described by nearly harmonic potential curves (see Table I). Therefore, the Franck-Condon transition matrix elements between the ground and intermediate states, $\langle n_i|n_o\rangle$, can be obtained from the corresponding C 1*s* photoelectron spectrum ($I \propto \langle n_i|n_o\rangle^2$ for direct photoionization). This method of obtaining the transition matrix elements between the ground and intermediate states has been used both at the shape resonance and far above.

IV. RESULTS AND DISCUSSION

The core photoelectron and the Auger decay spectra have been recorded at 305-eV photon energy at the maximum of the C 1*s* shape resonance and well above the two-electron excitation resonances [22]. At this photon energy a large shape-resonance-induced distortion of the vibrational progression can be expected. For comparison, the Auger decay spectrum and the C 1*s* photoelectron spectra have been recorded far above the threshold, where the influence of the shape resonance should be negligible.

A. The C 1*s* photoelectron spectra

The C 1*s* spectra recorded at 54.7° are presented in Fig. 1. There are clear differences between the spectra recorded at 305- and 330-eV photon energy. These differences can be explained in terms of two different threshold effects. First, the shape resonance is at a maximum at 305 eV and will affect the vibrational progression [5]. Second, PCI distorts the core photoelectron line shape close to threshold, affecting the 305-eV spectrum more than that measured at 330 eV. For photoelectron lines, PCI implies a shift towards lower kinetic energy, line broadening, and a low-energy asymmetric tail [23]. The spectra were fit with the EWA program package [24] using a PCI-distorted line profile. Correct implementation of the PCI effect is important since the asymmetric tail of the strongest vibrational level overlaps with the weaker vibrational levels. From the fit we obtained vibrational branching ratios of 100:62:15 for 330-eV photon energy and 100:83:25 for 305-eV photon energy, in reasonable agreement with the values reported by Randall *et al.* [5] ($\approx$100:62:13 and $\approx$100:89:33). From the present fits we also obtain a lifetime width estimate of 98(15) meV for the C 1*s* core-ionized state. This agrees with published values of 90(15) meV [5], 97(10) meV [19], and 78(10) meV [11]. No

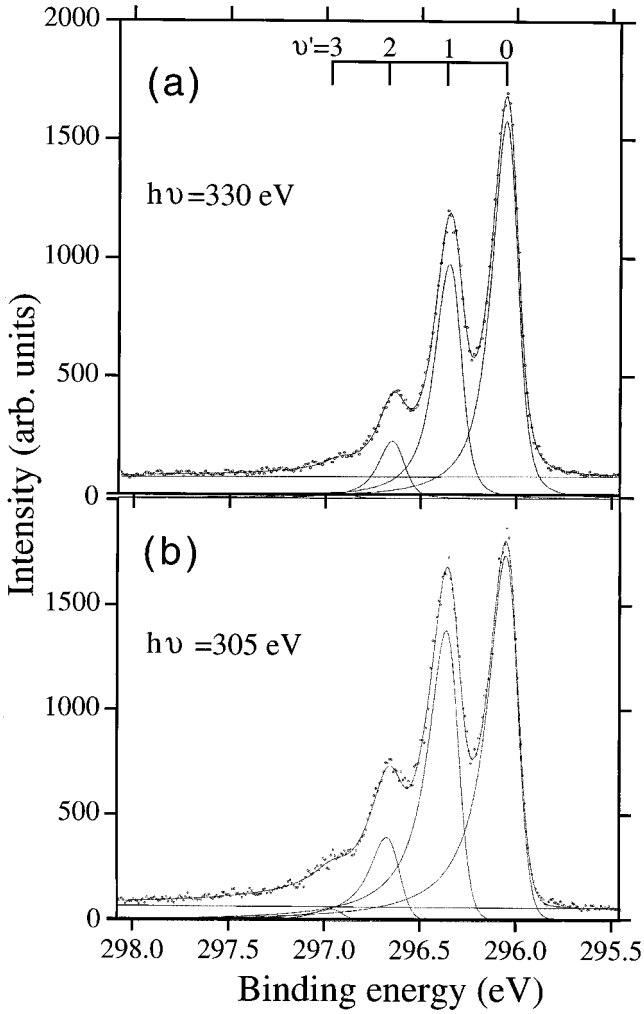

FIG. 1. CO C 1*s* photoelectron spectra (dotted) recorded at 54.7° and a photon energy of 305 eV (a) and 330 eV (b). The solid line shows a PCI fit to the experimental data.

variations in lifetime broadening between the spectra measured at 305 and 330 eV were found within the error bars. The branching ratios and the lifetime width extracted from the fits were used as input to the calculations of the Auger decay spectra.

B. The Auger decay spectra

The ground-state configuration of CO is (core) $(3\sigma)^2(4\sigma)^2(1\pi)^4(5\sigma)^2$. In Fig. 2 the experimental Auger decay spectra are presented together with the calculated spectra. The deexcitation of the C $1s^{-1}$ intermediate core-hole state populates predominantly three electronic final states in the kinetic energy region shown in Fig. 2: the *X* state, which has a $(5\sigma^{-2})$ leading configuration, the *A* state $(5\sigma^{-1}1\pi^{-1})$ and the *B* state $(5\sigma^{-1}4\sigma^{-1})$. All of these final states are of singlet spin configuration; in principle, the corresponding triplet states also exist in this energy region but previous studies have shown that the intensity of these triplet states is at least an order of magnitude lower than that of the corresponding singlet states [21,25]. Therefore, the following discussion will be restricted to the *X*, *A*, and *B* states of singlet spin configuration.

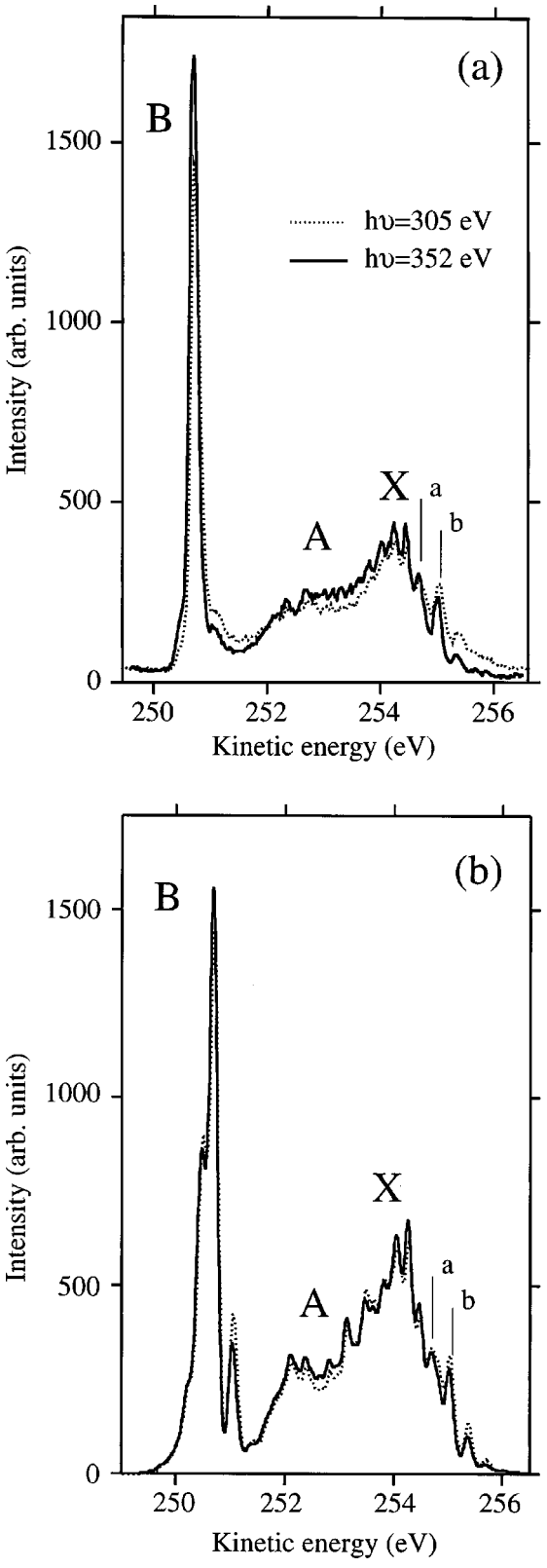

FIG. 2. (a) Experimental Auger decay spectra from the core-ionized C $1s^{-1}$ state of CO. The solid line represents the spectra recorded with a photon energy of 305 eV at the maximum of the C 1*s* shape resonance and the dotted line is for the spectra recorded at a photon energy of 352 eV. (b) Calculations, following the conventions of (a). Both experimental and simulated spectra are normalized so that the total intensity is the same at the shape resonance and far above.

There are obvious differences between the spectra recorded at the shape resonance and far above. However, before discussing the differences in terms of the shape resonance, it should be stressed that, similar to the C 1*s* spectra, the PCI effect influences the Auger decay spectrum recorded at 305-eV photon energy more severely than the Auger decay spectrum recorded at 352 eV. In order to examine this, additional Auger decay spectra were recorded with photon energies of 298 and 301 eV, i.e., just above the C 1*s* ionization threshold at 296 eV where the influence of PCI is large and the shape resonance is very weak. It was observed that even though PCI clearly influences the intensity distribution, the large differences between the spectra of Fig. 2 could not be reproduced. We thus conclude that the differences between the spectra recorded at 305- and 352-eV photon energies are attributed mainly to the C 1*s* shape resonance. The most evident differences between the spectra in Fig. 2(a) are found at the high-kinetic-energy side of the *X* state. In particular, there are two lines marked ''*a*'' and ''*b*'' in Fig. 2. While in the spectrum recorded at 352 eV, line ''*a*,'' is more intense, an almost equal intensity is observed in the spectrum recorded at 305 eV. We are inclined to attribute the difference to a modified vibrational envelope of the intermediate state, since the population of $\nu'=1,2$ vibrational levels is increased at the shape resonance; see Fig. 1. In one of our previous studies of the resonant Auger decay spectra recorded at the C $1s\rightarrow 3p$ resonance, it was found that the ''*a*'' level was predominantly populated by the $3p$ ($\nu'=0$) level and the ''*b*'' level by the $3p$ ($\nu'=1,2$) levels [16]. Such a comparison is justified, since the vibrational progression in the resonant Auger decay spectrum at the C $1s\rightarrow 3p$ resonance shows clear similarities to the Auger decay spectrum of the C 1*s* core-ionized state. A further difference between the spectra recorded at maximum and far above the shape resonance is the lower intensity of the main line of the *B* state at the shape resonance. The main line of the *B* state is due to transitions between levels of the same vibrational quantum number of the intermediate and final state, i.e., $\Delta\nu=0$. The potential curve of the *B* state supports only three vibrational levels. Since the internuclear equilibrium distance is similar to the core-ionized intermediate state; this enhances the $\Delta\nu=0$ transition [26]. Within the Franck-Condon description of the deexcitation, it is reasonable to assume that the higher vibrational levels of the intermediate state are most likely to decay to the dissociative part of the *B* state potential curve. Transitions to the dissociative part are located at the high-kinetic-energy side of the $\Delta\nu=0$ line. This would explain not only the lower intensity of the $\Delta\nu=0$ line in the spectrum recorded at the shape resonance, but also the higher intensity in the 251–252-eV kinetic-energy region. However, the increase of intensity in the 251–252-eV kinetic-energy region is also enhanced by PCI.

The previous two examples show that the modified vibrational population of the intermediate state is important in order to explain the Auger decay spectrum at the shape resonance. In the following, numerical simulations will be used to show quantitatively that the influence of the shape resonance on the Auger vibrational progression can be understood only by the increased population of higher vibrational levels in the intermediate state. Thus the temporary trapping

of the photoelectron at the shape resonance has little or no influence on the deexcitation step. The simulations have been carried out applying the formalism presented in Sec. III. Morse potential curves have been used for both the intermediate and the final states. The spectroscopic constants used to calculate the Morse curves of the core-ionized intermediate state together with the *X* and the *A* final state have been taken from Correia *et al.* [21] whereas values for the *B* state are from Larsson *et al.* [26]. These values are summarized in Table I. The results of the simulations are presented in Fig. 2(b). Reasonably good agreement between these simulations and the experimentally obtained spectra of Fig. 2(a) is found for the *A* and *X* final states. For the *B* state there are obvious differences. These differences stem most probably from the simple Morse potential curve, which is not able to reproduce the complicated *B* state potential curve. The *B* state potential curve has double minima due to a forbidden crossing, where the inner part supports only three vibrational levels [21,26]. Even though the Morse curve can partly describe the inner part of the *B* state, if the anharmonicity constant is large, more advanced treatment of this potential curve seems necessary.

When comparing the two simulated Auger decay spectra in Fig. 2(b), it is seen that the main differences between the experimentally obtained spectra are reproduced in the simulated spectra, particularly for transitions to the *X* and *A* final states. For instance, the previously discussed differences between line ''*a*'' and ''*b*'' and the lower intensity for the $\Delta\nu=0$ line in the *B* state are reproduced in the simulations. The intensity increase in the 251–252-eV region is not present in the simulated spectra due to limitations in the Morse potential. However, in the simulations the transitions with $\Delta\nu=\pm1$ increase at the shape resonance. In a more realistic description of the *B*-state potential curve these transitions would be more likely to populate the dissociative part than $\Delta\nu=0$, so we believe that this observation can also be explained by the simulation. It should be mentioned that the PCI effect has not been accounted for in the calculations. For Auger lines, the PCI effect causes an asymmetry towards high kinetic energy. This may partly explain some of the differences between the calculated and experimental spectra for the Auger decay at the shape resonance.

As mentioned above, no free parameters have been used in the simulations presented in Fig. 2(b). The only differences between the two simulated Auger decay spectra are the transition matrix elements from the ground to intermediate state, which are determined from the corresponding C 1*s* photoelectron spectra presented in Fig. 1. Due to the reasonably good ability of the simulations to account for the influence of the shape resonance, this indicates that the Auger decay spectrum from the shape resonance can be generally well understood by just a modified vibrational population of the intermediate core-ionized state. Contrary to the picture of a temporarily trapped electron, this finding indicates that the trapped electron does not influence the deexcitation step in the Auger process. This in turn implies that the characteristic time scale of the trapping should be shorter than the lifetime of the core-ionized intermediate state. Considering the relation between energy uncertainty and lifetime $\tau\delta E\approx\hbar/2$, this finding is in perfect agreement with the fact that the shape resonance is a couple of eV broad, whereas the C 1*s* lifetime width is only ≈0.1 eV in CO [5,6].

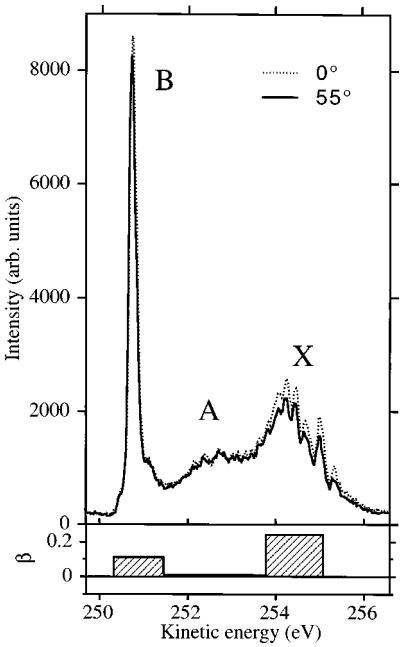

FIG. 3. Auger decay spectra recorded in the vicinity of the σ^* shape resonance, $h\nu=305$ eV. The solid line is for the spectrum taken at the magic angle of 54.7° and dotted line represents the spectrum recorded at 0° with respect to the electric vector of the incoming photon beam. The bars underneath the spectra represent the angular asymmetry parameter β.

C. Angular asymmetry in the Auger decay spectrum at the shape resonance

The Auger decay spectra presented in Fig. 3 have been recorded with 305-eV photon energy (corresponding to the maximum of the shape resonance) at both 0° and 54.7°. To account for the kinetic-energy dependence of the transmission of the spectrometer, the valence lines were recorded together with the Auger decay spectrum. Since the β values are known for the valence lines [27], these lines provide an inherent normalization of absolute intensity between spectra recorded at 0° and 54.7°. The whole Auger decay region in Fig. 3 has an average $\beta=0.10(5)$; a low positive β for this Auger group was also found in Ref. [27]. Taking advantage of the high resolution in the present recordings, it was possible to extract β values for transitions to specific final electronic states; $\beta=0.24(10)$ (X), $\beta=0.01(10)$ (A), and $\beta=0.11(10)$ (B). These values are also displayed in Fig. 3. In Ref. [16] we observed that transitions to the $X+3p$ state from the C $1s\rightarrow3p$ excited state has an angular anisotropy that varies with the vibrational level of the final state. Examining the finer details of Fig. 3, there is no obvious indication of a similar trend in the Auger decay spectrum from the shape resonance. One explanation for this could be that the C $1s\rightarrow3p$ excited states were prepared vibrationally selectively, while this is not possible for excitations at the shape resonance. Due to the presence of more than one vibrational level in the core-excited state, any vibrationally dependent asymmetry may be smeared out in the Auger decay spectrum. We cannot exclude that the coupling between the valence and $3p$ Rydberg electron is essential in order to give

rise to angular asymmetry depending on the vibrational level of the final state, as observed in Ref. [16].

V. CONCLUSIONS

We report measurements of the Auger decay spectrum from the C 1*s* shape resonance recorded with both angular and vibrational resolution. The primary observation is that vibrational structure in the Auger decay spectrum is affected by the shape resonance. To understand this finding, the experimental results have been compared to simulations based upon scattering formalism for Auger decay. The simulations show that the vibrational progressions affected by the shape resonance can be quantitatively understood as simply a modified population of the vibrational levels in the core-ionized intermediate state. This implies that the temporary trapping of the photoelectron at the shape resonance does not influence the deexcitation step. Therefore, we are inclined to conclude that the characteristic time scale of the trapping is shorter than the lifetime of the core-ionized intermediate state.

The angular distribution of the Auger decay of the shape resonance has been found to show a relatively weak dependence upon the final state. It was not possible to observe any difference in angular anisotropy for transitions to different vibrational levels within a final electronic state.

ACKNOWLEDGMENTS

The authors wish to thank the staff of the MAX laboratory for assistance during measurements. J.-O. Forsell is acknowledged for the design of the equipment. This work has been supported by the Nordic Academy for Advanced Study (NorFA) and the Swedish Natural Science Research Council (NFR). A.K. also thanks the Estonian Science Foundation for support.

[1] B. E. Cole, D. L. Ederer, R. Stockbauer, K. Codling, A. C. Parr, J. B. West, E. D. Poliakoff, and J. L. Dehmer, J. Chem. Phys. **72**, 6308 (1980).

[2] P. M. Dittman, D. Dill, and J. L. Dehmer, J. Chem. Phys. **76**, 5703 (1982).

[3] P. Roy, R. J. Bartlett, W. J. Trela, T. A. Ferrett, A. C. Parr, S. H. Southworth, J. E. Hardis, V. Schmidt, and J. L. Dehmer, J. Chem. Phys. **94**, 949 (1991).

[4] M. R. F. Siggel, M. A. Hayes, M. A. MacDonald, J. B. West, J. L. Dehmer, A. C. Parr, J. E. Hardis, I. Iga, and V. Tiit, J. Chem. Phys. **96**, 7433 (1992).

[5] K. J. Randall, A. L. D. Kilcoyne, H. M. Köppe, J. Feldhaus, A. M. Bradshaw, J.-E. Rubensson, W. Eberhardt, Z. Xu, P. D. Johnson, and Y. Ma, Phys. Rev. Lett. **71**, 1156 (1993).

[6] J. J. Rehr, R. C. Albers, and S. I. Zabinsky, Phys. Rev. Lett. **69**, 3397 (1992).

[7] J. L. Dehmer and D. Dill, Phys. Rev. Lett. **35**, 213 (1975).

[8] J. L. Dehmer, D. Dill, and S. Wallace, Phys. Rev. Lett. **43**, 1005 (1979).

[9] O. Hemmers, F. Heiser, J. Eiben, R. Wehlitz, and U. Becker, Phys. Rev. Lett. **71**, 987 (1993).

[10] A. Kivimäki, M. Neeb, B. Kempgens, H. M. Köppe, and A. M. Bradshaw, Phys. Rev. A **54**, 2137 (1996).

[11] H. M. Köppe, A. L. D. Kilcoyne, J. Feldhaus, and A. M. Bradshaw, J. Electron Spectrosc. Relat. Phenom. **75**, 97 (1995).

[12] J. A. Stephens and D. Dill, Phys. Rev. A **31**, 1968 (1985).

[13] V. Schmidt, Rep. Prog. Phys. **55**, 1483 (1992).

[14] S. Aksela, A. Kivimäki, A. Naves de Brito, O.-P. Sairanen, S. Svensson, and J. Väyrynen, Rev. Sci. Instrum. **65**, 831 (1994).

[15] S. Svensson, J.-O. Forsell, H. Siegbahn, A. Ausmees, G. Bray, S. Södergren, S. Sundin, S. J. Osborne, S. Aksela, E. Nõmmiste, J. Jauhiainen, M. Jurvansuu, J. Karvonen, P. Barta, W. R. Salaneck, A. Evaldsson, M. Lögdlund, and A. Fahlman, Rev. Sci. Instrum. **67**, 2149 (1996).

[16] S. Sundin, S. J. Osborne, A. Ausmees, O. Björneholm, S. L. Sorensen, A. Kikas, and S. Svensson, Phys. Rev. A **56**, 480 (1997).

[17] T. Åberg, Phys. Scr. **T41**, 71 (1992).

[18] T. Åberg and B. Crasemann, in *''Radiative and Radiationless Resonant Raman Scattering'' in X-ray Resonant (Anomalous) Scattering*, edited by G. Materlik, K. Fischer, and C. Sparks (Elsevier, Amsterdam, 1994).

[19] S. J. Osborne, A. Ausmees, S. Svensson, A. Kivimäki, O.-P. Sairanen, A. Naves de Brito, H. Aksela, and S. Aksela, J. Chem. Phys. **102**, 7317 (1995).

[20] The probability of finding the molecule in the lowest vibrational level, $\nu=0$, of the ground state is given by the Boltzmann distribution: $\rho_l=\exp(-E_l^0/k_BT)/\Sigma_l\exp(-E_l^0/k_BT)$. For the ground-state of CO the vibrational spacing is ≈ 270 meV [21]. At room temperature this implies that $\rho_o>99.9\%$.

[21] N. Correia, A. Flores-Riveros, H. Ågren, K. Helenelund, L. Asplund, and U. Gelius, J. Chem. Phys. **83**, 2035 (1985).

[22] M. Domke, C. Xue, A. Puschmann, T. Mandel, E. Hudson, D. A. Shirley, and G. Kaindl, Chem. Phys. Lett. **173**, 122 (1990).

[23] G. B. Armen, J. Tulkki, T. Åberg, and B. Crasemann, Phys. Rev. A **36**, 5606 (1987).

[24] J. Végh, *Ewa-data Analysis Program* (Institute of Nuclear Research of the Hungarian Academy of Sciences, Debrecen, Hungary, 1992).

[25] H. Ågren, J. Chem. Phys. **75**, 1267 (1981).

[26] M. Larsson, B. J. Olsson, and P. Sigray, Chem. Phys. **139**, 457 (1989).

[27] O. Hemmers, S. B. Whitfield, N. Berrah, B. Langer, R. Wehlitz, and U. Becker, J. Phys. B **28**, L693 (1995).